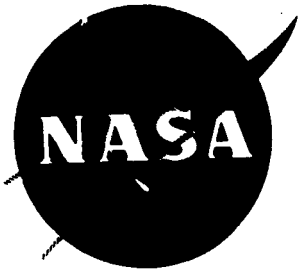

NASA CR-72053

FINAL REPORT

ELECTRON COLLISION CROSS SECTIONS IN METAL VAPORS

by

J. F. Nolan

prepared for

National Aeronautics and Space Administration

September 23. 1966

Contract NAS 3-7930

Technical Management
NASA Lewis Research Center
Cleveland, Ohio
Spacecraft Technology Division
N. J. Stevens

Westinghouse Research Laboratories
Atomic and Molecular Sciences R and D
Beulah Road, Churchill Borough
Pittsburgh, Pennsylvania 15235

NOTICE

This report was prepared as an account of Government sponsored work. Neither the United States, nor the National Aeronautics and Space Administration (NASA), nor any person acting on behalf of NASA:

A.) Makes any warranty or representation, expressed or implied, with respect to the accuracy, completeness, or usefulness of the information contained in this report, or that the use of any information, apparatus, method, or process disclosed in this report may not infringe privately owned rights; or

B.) Assumes any liabilities with respect to the use of, or for damages resulting from the use of any information, apparatus, method or process disclosed in this report.

As used above, "person acting on behalf of NASA" includes any employee or contractor of NASA, or employee of such contractor, to the extent that such employee or contractor of NASA, or employee of such contractor prepares, disseminates, or provides access to, any information pursuant to his employment or contract with NASA, or his employment with such contractor.

Requests for copies of this report should be referred to

National Aeronautics and Space Administration
Office of Scientific and Technical Information
Attention: AFSS-A
Washington, D.C. 20546

ELECTRON COLLISION CROSS SECTIONS IN METAL VAPORS

by

J. F. Nolan

ABSTRACT

The Townsend α coefficient has been measured in potassium-helium mixtures as a function of E/p, the ratio of electric field to total pressure, and N_K/N_{He}, the ratio of potassium to helium density. By comparing the measured values with the results of a numerical solution of the Boltzmann equation, one obtains cross sections consistent with the measurements. A total excitation cross section for potassium having a peak value of $1.0 \times 10^{-14} cm^2$ at 10 eV gives good agreement with experiment.

SUMMARY

Measurements of the Townsend α coefficient have been made in potassium-helium mixtures of various concentrations as a function of E/p, the ratio of the applied electric field to the total pressure, and also as a function of N_K/N_{He}, the ratio of potassium to helium density. From an analysis of the behavior of transport coefficients as a function of E/p, it is possible to deduce the collision cross section for electrons in the gas mixture as a function of electron energy. The analysis involves a numerical solution of the Boltzmann transport equation, so that no a priori assumptions about the shape of the electron energy distribution function are required. For low density ratios ($N_K/N_{He} < 10^{-4}$), the drift velocity is the same as that in pure helium at low E/p, indicating that elastic collisions between electrons and potassium atoms do not have a significant effect. However, the Townsend α coefficient is appreciably larger than in pure helium, indicating that inelastic collisions with potassium atoms are important even at these low density ratios. The Townsend α coefficient data have been analyzed to give a total excitation cross section for potassium consistent with these measurements and with previous measurements of the potassium ionization cross section. An excitation cross section with a peak value of $1.0 \times 10^{-14} cm^2$ at 10 eV gives good agreement with the experiments. Calculations indicate that at higher density ratios, elastic collisions between electrons and alkali metal atoms should cause the drift velocity to depart significantly from the value characteristic of pure helium; attempts to measure the drift velocity in cesium under these calculations were made, but the data could not be analyzed due to experimental difficulties.

I. INTRODUCTION

Electron swarm techniques have proven to be quite useful for obtaining electron-atom collision cross sections at low energies. Recent measurements in this laboratory have yielded the cross section for electron-cesium atom inelastic collisions.[1,2] The present report describes the continuation of this work and the extension of the cross section measurements to potassium.

In general, the present method of obtaining cross sections involves the measurement of some transport coefficient for electrons under the influence of an applied electric field in a gas at high pressure. Typical examples of transport coefficients are the electron drift velocity and Townsend α coefficient. These quantities are measured as a function of E/p, the ratio of applied electric field to gas pressure. For a given value of E/p, the electrons have a relatively broad distribution in energy; i.e., the spread in energy is comparable to the mean energy. This results in the fact that the transport coefficient depends on the collision cross section through an average over the electron energy distribution function. Consequently in order to obtain the cross section as a function of energy, it is necessary to know the shape of the electron energy distribution function. This is accomplished through a numerical solution of the Boltzmann transport equation.

The measurements described in the present work were carried out in mixtures of potassium and helium. In principle one could obtain the potassium cross section by making measurements in pure potassium vapor at high pressures. However, in practice such measurements are extremely difficult because of the corrosive properties of alkali metal vapors, particularly on electrical insulators. These difficulties can be minimized by working with mixtures in which the alkali is a minor constituent. Helium is used as the major constituent because the cross sections for electron-helium collisions are well known.

II. APPARATUS

The vacuum system used for these measurements is similar to that employed previously[2]. Fig. 1 shows a schematic drawing of the system. The measurements are made in the drift tube, which is contained in the main oven. The portion of the system inside the main oven (and extending for a short distance outside the main oven) is fabricated of stainless steel; typically, this part of the system operates at $\sim 300^{\circ}C$. The portion of the system outside the oven is constructed mainly of glass; except for initial bake-out, this part of the system operates at room temperature. The vacuum system is provided with a Bayard-Alpert ionization gauge for measuring the pressure of the residual vacuum, a null indicating capacitance manometer for measuring high pressures (> 1 Torr), and a supply of high purity helium.

Before the alkali metal is introduced into the system, the entire system is baked out at $\sim 400^{\circ}C$ for about 24 hours to insure a low background pressure. Typically, the background pressure is 2×10^{-9} Torr, with a rate of rise of 2×10^{-9} Torr/min. with the system valved off from the pumps. When a good residual vacuum has been obtained the alkali metal is introduced into the system. Under normal operation the alkali metal is contained in the liquid metal reservoir (shown in Fig. 1). The reservoir consists of a length of stainless steel tubing extending down from the drift tube and closed off at the lower end. The reservoir extends through the base of the main oven into a separate oven, designated the reservoir oven in Fig. 1. The temperature of the reservoir oven determines the alkali vapor pressure in the drift tube. The temperature of the reservoir oven is always less than that of the main oven.

The mechanism for initial introduction of the alkali metal into the system has been modified from that used in the past. Previously the alkali was contained in a glass ampule and was admitted to the system by breaking the ampule;

in the present version the alkali is contained in a metal ampule and is admitted to the system by rupturing a thin diaphragm in the metal ampule. This change was necessary to prevent the alkali from being destroyed in a chemical reaction with the glass at high temperatures. A schematic drawing of the metal ampule is shown in Fig. 2. It consists of a stainless steel cylindrical container 3-3/4 inches long by 0.705 inches O.D., closed off at the bottom end. The central section of the closed off end consists of a thin stainless steel diaphragm (0.005 inches thick). A 3/16 inch O.D. Kovar tube leads away from the upper end of the cylinder; the alkali metal is transferred from the glass ampule supplied by the manufacturer to the metal ampule through the Kovar tubing. When the metal ampule has been filled, the Kovar tube is pinched-off to give a vacuum-tight seal. After pinch-off, the seal is welded to prevent the pinch-off seal from opening up at high temperatures. The system used for transferring the alkali from the glass to the metal ampule is also equipped with a supply of helium gas. After the alkali has been transferred to the metal ampule, helium is admitted to the system to a pressure of several Torr. The reason for this is that after the Kovar has been pinched-off and welded, the seal can be checked with a helium leak detector to see if any helium is leaking out; if no helium leaks out with the other side evacuated, than the pinch-off seal is vacuum tight. The alkali is introduced into the system by forcing the thin diaphragm in the metal ampule against a sharp Inconel spike. This motion is made possible by a bellows arrangement in the vacuum wall of the outer stainless steel cylinder. When the diaphragm is pierced the reservoir tube is cooled to a temperature lower than that of any other part of the system so that the alkali metal will condense into the reservoir. The path from the ampule to the alkali reservoir is down hill, so that the transfer of the alkali metal is assisted by gravity.

The main elements in the drift tube are two parallel plate electrodes made of Advance (nickel-copper alloy). One of the electrodes has a guard ring around the outside to ensure that the applied electric field is uniform in the central region. The split structure of this electrode may be seen in Fig. 3, which shows a photograph of the electrode region of the drift tube. Electric fields are applied by applying a voltage to the unguarded electrode (hereafter called the cathode). Currents are measured to the central disc of the guarded electrode (hereafter called the anode). The spacing between the two electrodes can be continuously varied between 0.05 and 1 cm through a bellows arrangement in the vacuum wall. The materials used for electrical insulation in the drift tube were single crystal sapphire and high purity polycrystalline aluminum oxide.

The electronic circuitry required for measurements of the Townsend α coefficient is quite simple. A regulated dc voltage supply is connected between the cathode and ground. The anode is always very nearly at ground potential, so the applied field is given by the applied voltage divided by the spacing between electrodes, provided that the current level is low enough so that space charge distortion of the applied field is negligible. The voltage supply is capable of providing voltages up to 1000 volts. However, for the conditions under which the measurements are made, the breakdown voltage to the gap is always less than 1000 volts, so that the largest value of the voltage applied is determined by the breakdown characteristics of the gap. Since the value of the breakdown voltage depends on the electrode spacing and the potassium and helium pressure, it changes as these parameters are varied. A typical value is 250 volts.

The anode current is determined by measuring the voltage developed across a known precision load resistor connected between the anode and ground. This voltage is always less than a few millivolts, and is usually in the microvolt region. Since the applied voltage is always greater than 1 volt, the anode may be considered to be at ground potential for purposes of calculating the applied

field. The current measured at the anode is in the range 10^{-11} to 10^{-6} Amperes.

III. METHOD OF MEASUREMENT AND RESULTS

For a uniform dc electric field applied between parallel plates, the prebreakdown current as a function of distance is given by[3]

$$I(x) = \frac{I_o \exp \alpha (x-x_o)}{1 - (\exp \alpha (x-x_o) - 1)} \qquad (1)$$

where I_o is the initial current at $x = o$, x is the distance from the electrode which acts as a current source, x_o is related to the distance which electrons must travel before an equilibrium velocity distribution is attained, γ is a generalized coefficient referring to electron production due to secondary processes, and α is the Townsend α coefficient. x_o is related to the electron mean free path and, for the high pressures used in the present measurements, may be safely taken as zero. If, in addition, secondary processes are not important, the above reduces to

$$I(x) = I_o \exp (\alpha x) \qquad (2)$$

so that α may be obtained by measuring I/I_o as a function of x. Experimentally, one may determine whether or not secondary processes are important by plotting $\ln (I/I_o)$ versus x. If secondary effects are important, the curves will bend upward; if not, straight lines will be obtained.

In the present case the initial current is supplied by thermionic emission from the potassium coated electrodes at the equilibrium temperature of the tube ($\sim 300^{o}C$). Since both electrodes are emitting, the prebreakdown current may be observed in either direction simply by reversing the polarity of the applied voltage. The initial current, I_o, cannot be measured directly, but it may be obtained by indirect methods described elsewhere.[2,4]

For a given value of E/p the variation of the current with inter-electrode spacing is given by Eq. (2) (or by Eq. (1) if secondary processes are not negligible). As E/p is changed the variation of current with distance will have the same form, but will be characterized by a different value of α. The object is to measure α as a function of E/p by observing the variation of ℓn $(I(x)/I_o)$ with x for different values of E/p. The value of α obtained will depend on the helium pressure and the potassium pressure in the drift tube, and in evaluating the data it is necessary to know these pressures. Since in these measurements the ratio of potassium pressure to helium pressure is small (10^{-4} or less), the helium pressure is equal to the total pressure to a good approximation. The helium pressure is obtained from the measurement of the total pressure with the capacitance manometer. Since the measurements are carried out over a range of gas temperatures, it is desirable to normalize the pressure to the equivalent pressure at some standard temperature. In the present work, $300^{o}K$ is chosen as the standard temperature and all pressure measurements are converted to P_{300}, the equivalent pressure at $300^{o}K$. The equivalent pressure is given by

$$P_{300} = P_T \left(\frac{300}{T}\right) \qquad (3)$$

where P_T is the pressure measured at temperature $T\ ^{o}K$. The gas density is given by

$$N = 3.22 \times 10^{16} P_{300} \qquad (4)$$

where N is in cm^{-3} and P_{300} is in Torr. The potassium vapor pressure was calculated from the expression given by Nesmeyanov[5]

$$\log_{10} P = 13.83624 - 4857.90/T + 0.00034940T - 2.21542 \log_{10} T \qquad (5)$$

where p is the vapor pressure in Torr and T is the temperature of the reservoir in ^{o}K.

The procedure used in obtaining a mixture was to admit helium to the desired pressure, set the reservoir temperature to give the desired potassium pressure, and close the isolating valve (Fig. 1). With the isolating valve closed, the vapor pressure of potassium in the drift tube at equilibrium is determined by the reservoir temperature; i.e. it is given by Eq. (5). To make sure that the measurements are characteristic of an equilibrium mixture, the α coefficient is measured as a function of time after closing the isolating valve. The measurements presented here are the long-time, equilibrium values.

The procedure used in measuring the α coefficient was to measure the current ratio, I/I_o, for several values of electrode spacing for a given value of E/p. This was then repeated for other values of E/p. The results of the measurements are presented as a function of E/p_{300}, where p_{300} is given by Eq. (3) and E = V/d, where V is the applied voltage and d is the spacing between electrodes. In taking measurements one must be sure that the current is small enough that space charge fields are negligible compared to the applied field. This point was checked by measuring the α coefficient as a function of the initial current, I_o, all other parameters being held constant. If space charge effects are not negligible, the value obtained for α will depend on the initial current. Space charge effects were negligible for the results presented here.

Fig. 4 shows the results obtained for α/p_{300} as a function of E/p_{300} for a potassium-helium mixture with a total normalized pressure of p_{300} = 365 Torr, and a density ratio $N_K/N_{He} = 2.11 \times 10^{-5}$. The points represent experimental measurements; the curve represents the values of α/p_{300} calculated on the basis of an assumed potassium excitation cross section. Also shown is the calculated contribution of Penning effect ionization to the α coefficient. These calculations are discussed in the next section. The error bars for the experimental points in Fig. 4 represent the probable error calculated from five different measurements on five separate days.

In addition to the measurements in potassium-helium mixtures described above, some measurements were also made in cesium-helium mixtures. The electron drift velocity was measured in the E/p_{300} range 0.02 to 0.3 volts/cm-torr, using the same technique as described previously.[2] Data was obtained for a mixture with a helium pressure of 148.6 Torr and with a cesium reservoir temperature of 562°K, which corresponds to a cesium vapor pressure of 1.41 Torr. The calculated density ratio for this mixture is $N_{Cs}/N_{He} = 9.50 \times 10^{-3}$. This is large enough so that the drift velocity should be significantly smaller (by a factor of two or more) than that characteristic of pure helium, because of the effect of elastic electron-cesium collisions. However, the results of drift velocity measurements in this mixture agreed quite accurately with the known drift velocity in pure helium. This surprising result was later understood when the system was dismantled and it was found that there was no cesium in the reservoir. Most of the cesium was destroyed by chemical reaction with the glass ampule used for initial introduction of the alkali into the system. Consequently the density ratio for the mixture was significantly less than the value 9.50×10^{-3} calculated from the reservoir temperature. The measurements referred to above were thus at some lower, unknown density ratio and it is not surprising that they agree with the pure helium drift velocity. Since the density ratio was lower than desired, these measurements gave no new information on the electron-cesium momentum transfer cross section. They did indicate the necessity of modifying the system such that no glass comes in contact with the alkali metal at high temperatures ($> 350^{\circ}C$). This was the reason for changing to the metal ampule

described above. Since the glass ampule has been replaced by the metal ampule, no problems involving loss of alkali by chemical reaction have been encountered.

IV. ANALYSIS OF DATA

The analysis of the data in the present case is similar to that presented previously[2] and will only be outlined here, without going into great detail. It is desired to obtain the potassium excitation cross section as a function of electron energy from the measurements of the Townsend α coefficient as a function of E/p_{300}. Since the α coefficient depends on the cross section through an average over the electron energy distribution function, it is necessary to know the form of the distribution function to obtain the cross section. The problem is that one does not know, a priori, the form of the distribution function since this depends, in part, on the cross section one is attempting to find. The procedure followed is to assume an excitation cross section, with proper threshold, as a function of electron energy and to use this cross section in obtaining a numerical solution of the Boltzmann equation. This gives the distribution function appropriate to the assumed cross section, so that the Townsend α coefficient can then be calculated as a function of E/p. This calculated α coefficient is then compared to the experimental values, and the input cross section is adjusted in magnitude and shape until the calculated and experimental α coefficients agree. This allows one to obtain a cross section which is consistent with the experimental results. The final cross section obtained in this way is not unique in that rapid changes with energy in the cross section curve will be at least partially averaged out because of the relatively large spread in the electron energy distribution.

For E/p_{300} less than 2.0 Volts/cm-Torr, inelastic collisions involving helium may be neglected and this range of E/p_{300} one need consider only inelastic collisions with potassium and elastic collisions with helium. Because of the low potassium to helium density ratios, elastic collisions with potassium may be neglected.[2] Thus, for E/p_{300} less than 2.0 Volts/cm-Torr, the Townsend α coefficient depends on three cross sections: the electron-helium momentum-transfer cross section, the electron-potassium ionization cross section, and the electron-potassium excitation cross section. If two of these are known, the third may be obtained by the method outlined above. In the present analysis the helium momentum transfer cross section and the potassium ionization cross section are taken to be known, and the measurements are used to determine the potassium excitation cross section. The helium momentum transfer cross section used in the analysis is taken from the work of Frost and Phelps.[6] See Figure 5a. The potassium ionization cross section used is shown in Fig. 5b. The energy dependence of this cross section is based on the measurements of Tate and Smith.[7] The absolute value is taken to be $8.0 \times 10^{-16} cm^2$ at the maximum of the cross section; this value is based on the work of McFarland and Kinney,[8] who report a maximum cross section of $8.2 \times 10^{-16} cm^2$. The potassium excitation cross section which gives best agreement with the present measurements is shown as the solid curve in Fig. 4; it is seen that the agreement with the measured values is good.

For E/p_{300} greater than 2.0 Volts/cm-Torr there is a contribution to the α coefficient from Penning effect ionization; i.e., metastable helium atoms are formed by electron impact and some of these metastables give up their excitation energy to ionize potassium atoms on collision. The contribution of Penning effect ionization to the α coefficient is shown in Fig. 4. It is seen that good agreement with experiment is obtained if it is assumed that 70% of the helium metastables formed are destroyed by Penning effect collisions. In calculating the Penning effect ionization, it is necessary to know the excitation and ionization cross sections. The helium excitation cross section used is based on the measurements of Maier-Leibnitz,[9] and the helium ionization cross section is taken

from Smith.[10]

Examples of calculated electron energy distribution functions are shown in Fig. 7 for two values of E/p_{300}. It will be seen that the actual distribution function falls off more rapidly with energy than does a Maxwellian distribution function.

DISCUSSION

The total potassium excitation cross section obtained in the present work may be compared with two recent measurements of the cross section for 4S-4P excitation as determined by optical techniques. It is expected that for potassium the cross section for 4S-4P excitation will be large compared to the cross section for excitation to higher states, so that the 4S-4P cross section should be nearly equal to the total excitation cross section. The reasons for this are the same as those previously advanced for the case of cesium.[1]

The cross section for 4S-4P excitation in potassium has been measured by Volkova and Devyatov,[11] and by Zapesochnyi and Shimon.[12] Fig. 8 gives a comparison of the results of these measurements with the present results. Volkova and Devyatov measured separate cross sections for the two components of the doublet, i.e. for excitation from the ground state to the $4\ P_{1/2}$ and $4\ P_{3/2}$ states. The curve labeled Volkova and Devyatov in Fig. 8 is the sum of these two cross sections. It is seen that the cross section derived from the present work is larger than that found by Zapesochnyi and Shimon, as was the case in cesium, and is smaller than that found by Volkova and Devyatov.

A theoretical calculation of the potassium excitation cross section has been reported by Vainshtein, et al.[13] This theoretical cross section is compared with the present experimental results in Fig. 10. It is seen that the curve of Vainshtein, et al. lies considerable below the experimental curve. This was also the case for the cesium excitation cross section.

1. J. F. Nolan and A. V. Phelps, Phys. Rev. 140, A792 (1965).

2. J. F. Nolan, Summary Report, Electron Collision Cross Sections in Metal Vapors, NASA CR-54670, Jan. 26, 1966.

3. A. von Engle, Handbuch der Physik, Edited by S. Flugge (Springer-Verlag, Berlin, 1956), Vol. XXI, p. 504.

4. R. W. Crompton, J. Dutton, and S. C. Haydon, Proc. Phys. Soc. (London), 869, 2 (1956).

5. A. N. Nesmeyanov, "Vapor Pressure of the Chemical Elements," (Elsevier Publishing Co., Amsterdam, 1963).

6. L. S. Frost and A. V. Phelps, Phys. Rev. 136, A1538 (1965).

7. J. T. Tate and P. T. Smith, Phys. Rev. 46, 773 (1934).

8. R. H. McFarland and J. D. Kinney, Phys. Rev. 137, A1058 (1965).

9. H. Maier-Leibnitz, Z. Phys. 95, 499 (1935).

10. P. T. Smith, Phys. Rev. 36, 1293 (1930).

11. L. M. Volkova and A. M. Devyatov, Bull. Acad. Sci. USSR, 27, 1025 (1963).

12. I. P. Zapesochnyi and L. L. Shimon, IVth International Conf. on the Physics of Electronic and Atomic Collisions, Aug. 1965, p. 401.

13. L. Vainshtein, V. Opyktin and L. Presnyakov, Soviet Physics JETP, 20, 1542 (1965).

Figure Captions

Fig. 1 Schematic diagram of vacuum system

Fig. 2 Metal ampule used for introduction of alkali metal into system. The thin stainless steel diaphragm is pierced by a sharp inconel spike (not shown).

Fig. 3 Detail of electrode region of drift tube, showing split structure of electrode. Currents are measured to the central disc; the outer guard ring is used to maintain uniformity of the applied electric field in the central region.

Fig. 4 α/p_{300} versus E/p_{300} for $N_K/N_{He} = 2.11 \times 10^{-5}$. The points are experimental measurements. The curve labeled "direct" is calculated using the potassium excitation cross section shown in Fig. 6.

Fig. 5a Momentum transfer cross section for electrons in helium.

Fig. 5b Potassium ionization cross section used in the analysis of the data. This cross section is based on references 7 and 8.

Fig. 6 Potassium excitation cross section obtained from the present measurements.

Fig. 7 Electron energy distribution functions for two values of E/p_{300}. Also shown for comparison is a Maxwellian distribution function (dotted curve) with a peak energy equal to that of the calculated distribution function for $E/p_{300} = 3.0$ Volts/cm-Torr.

Fig. 8 Comparison of the total potassium excitation cross section derived from the present work with the cross section for 4S-4P excitation as found by Volkova and Devyatov (reference 11) and by Zapesochnyi and Shimon (reference 12).

Fig. 9 Comparison of the theoretical cross section for 4S-4P potassium excitation as found by Vainshtein et al (reference 13) with the present results.

Dwg. 746A571

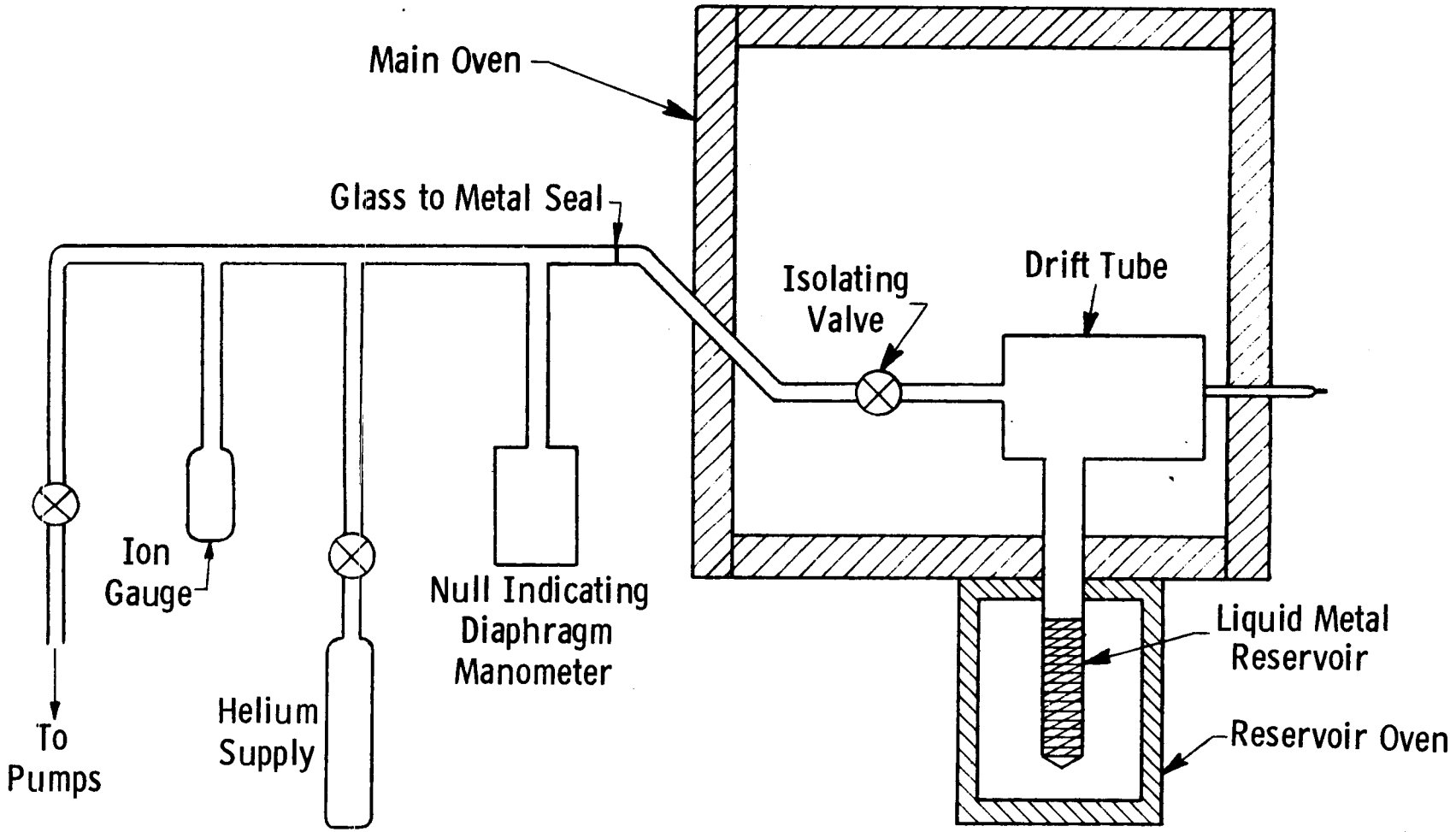

Figure 1 Schematic Diagram of vacuum system

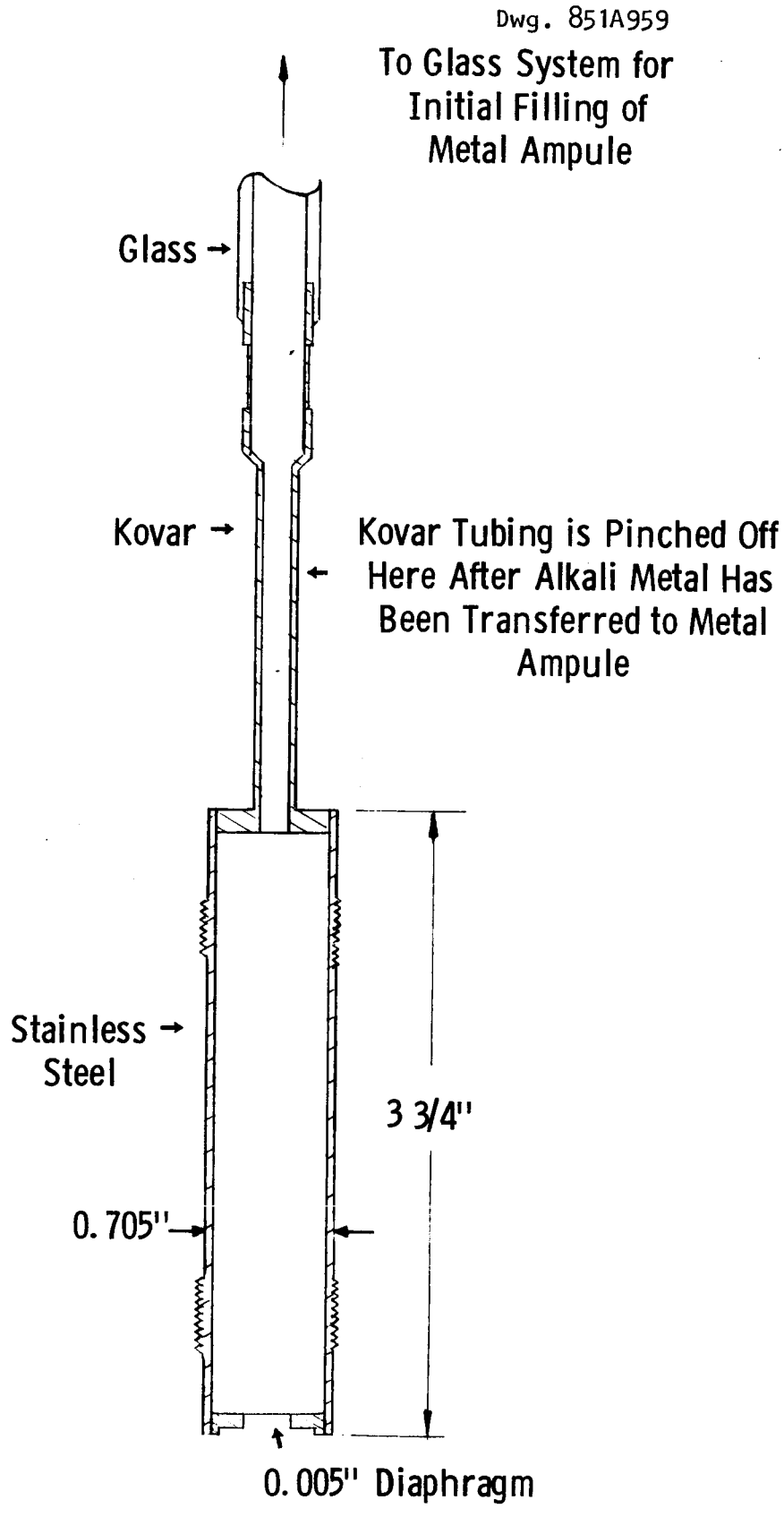

Fig. 2 Metal ampule used for introduction of alkali metal into system. The thin stainless steel diaphragm is pierced by a sharp inconel spike (not shown).

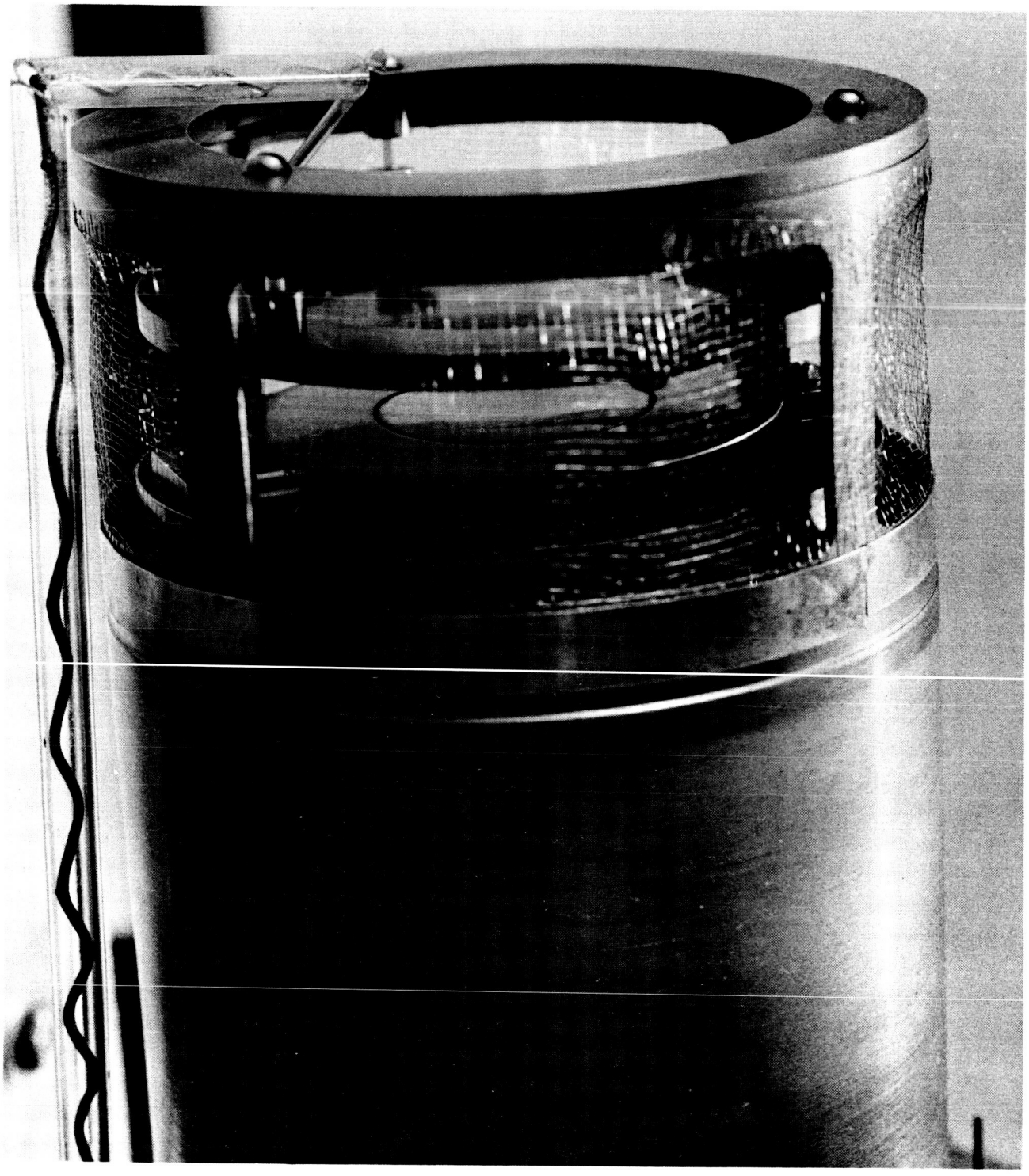

Fig. 3 Detail of electrode region of drift tube, showing split structure of electrode. Currents are measured to the central disc; the outer guard ring is used to maintain uniformity of the applied electric field in the central region.

Fig. 4 α/p_{300} versus E/p_{300} for $N_K/N_{He} = 2.11 \times 10^{-5}$. The points are experimental measurements. The curve labeled "direct" is calculated using the potassium excitation cross section shown in Fig. 6.

CURVE 570890-A

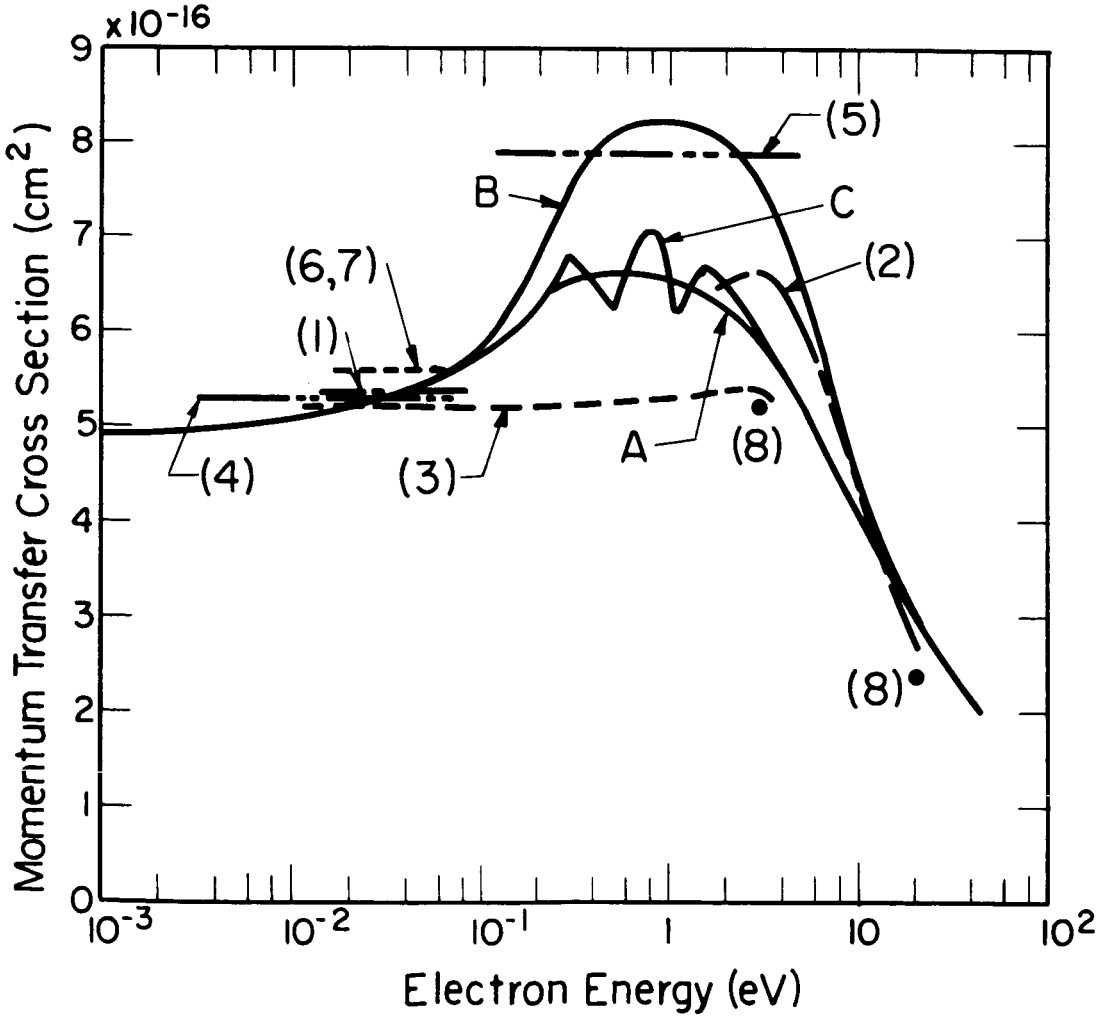

Fig. 5a Momentum transfer cross section for electrons in helium.

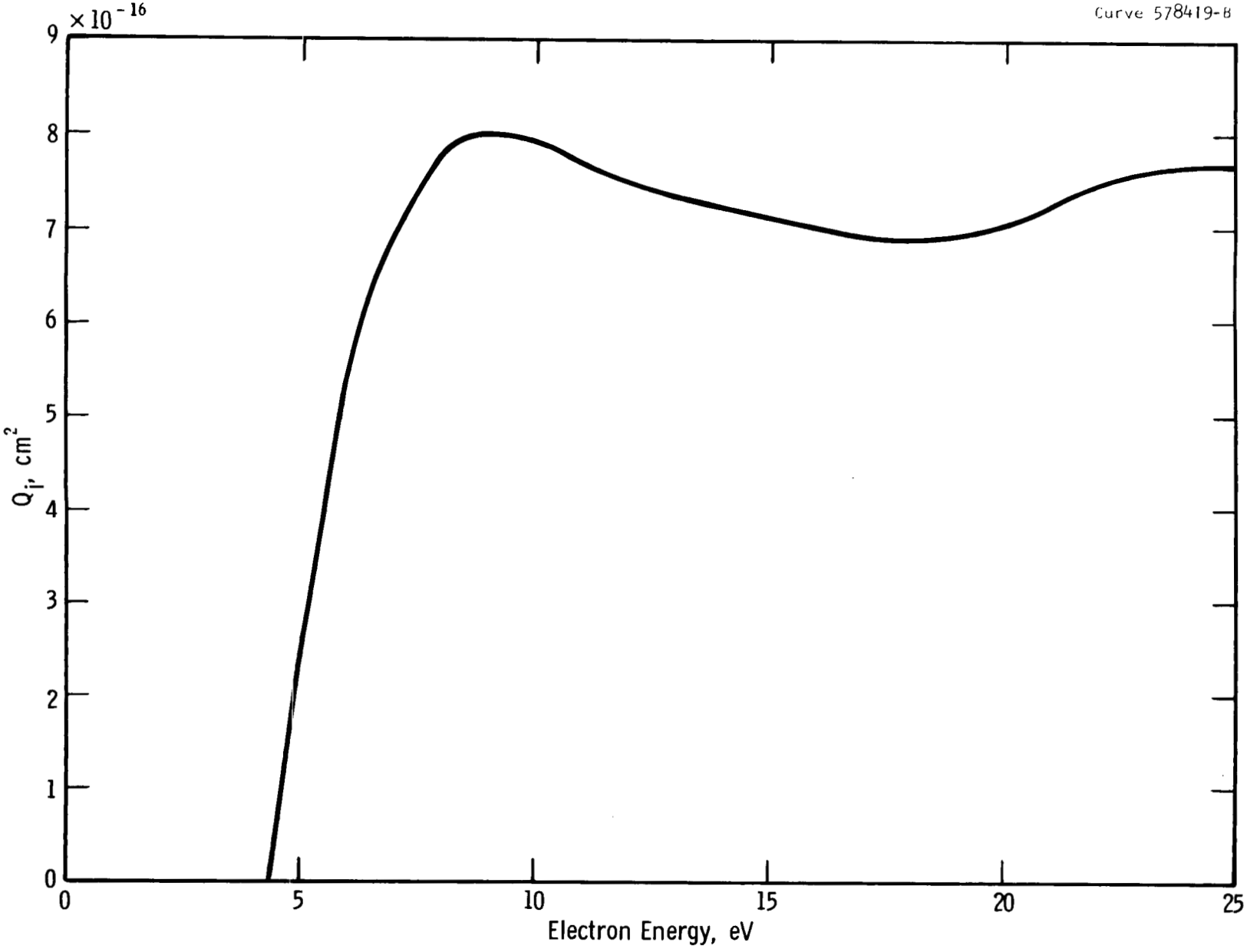

Fig. 5b Potassium ionization cross section used in the analysis of the data. This cross section is based on references 7 and 8.

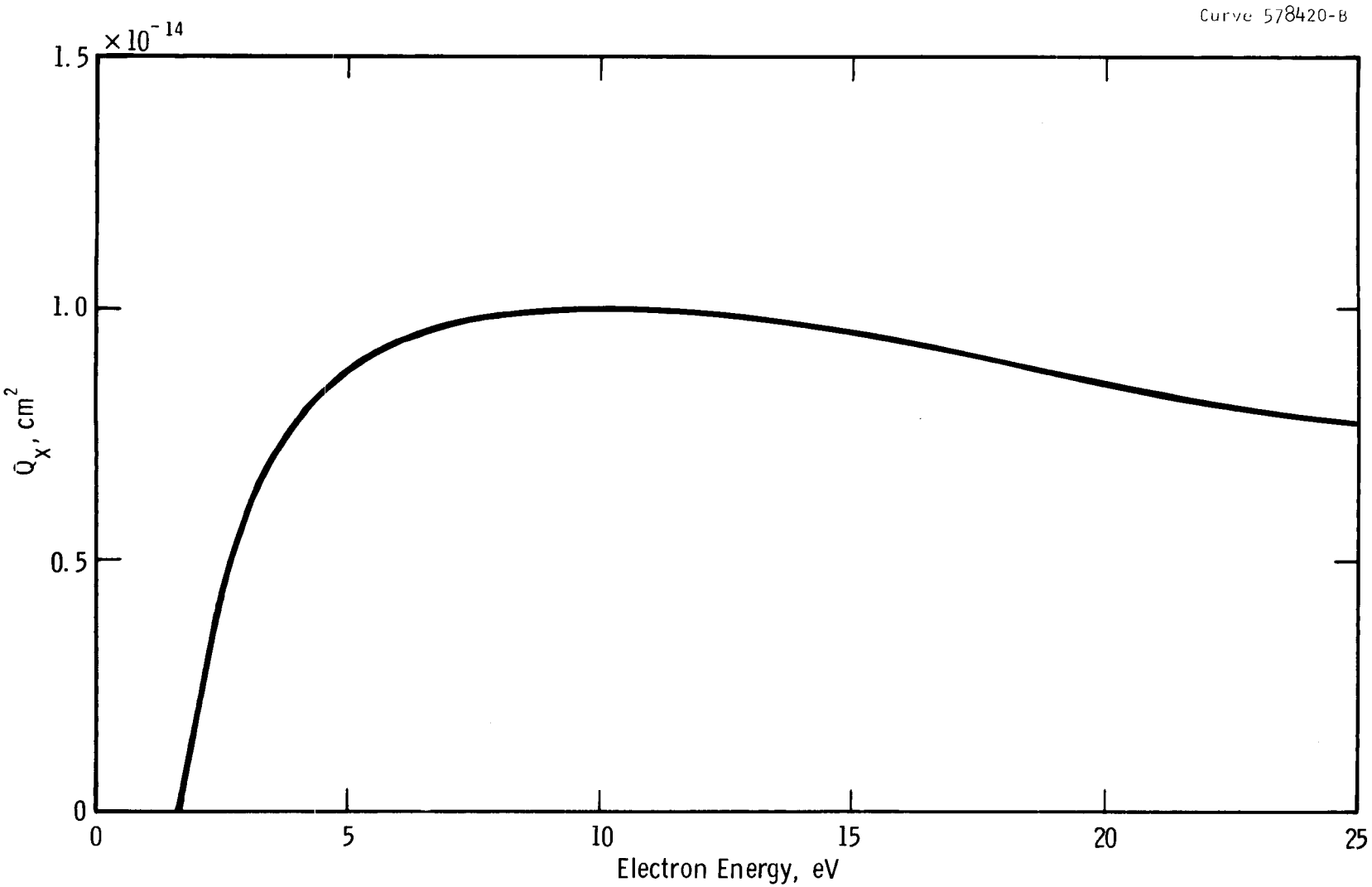

Fig. 6 Potassium excitation cross section obtained from the present measurements.

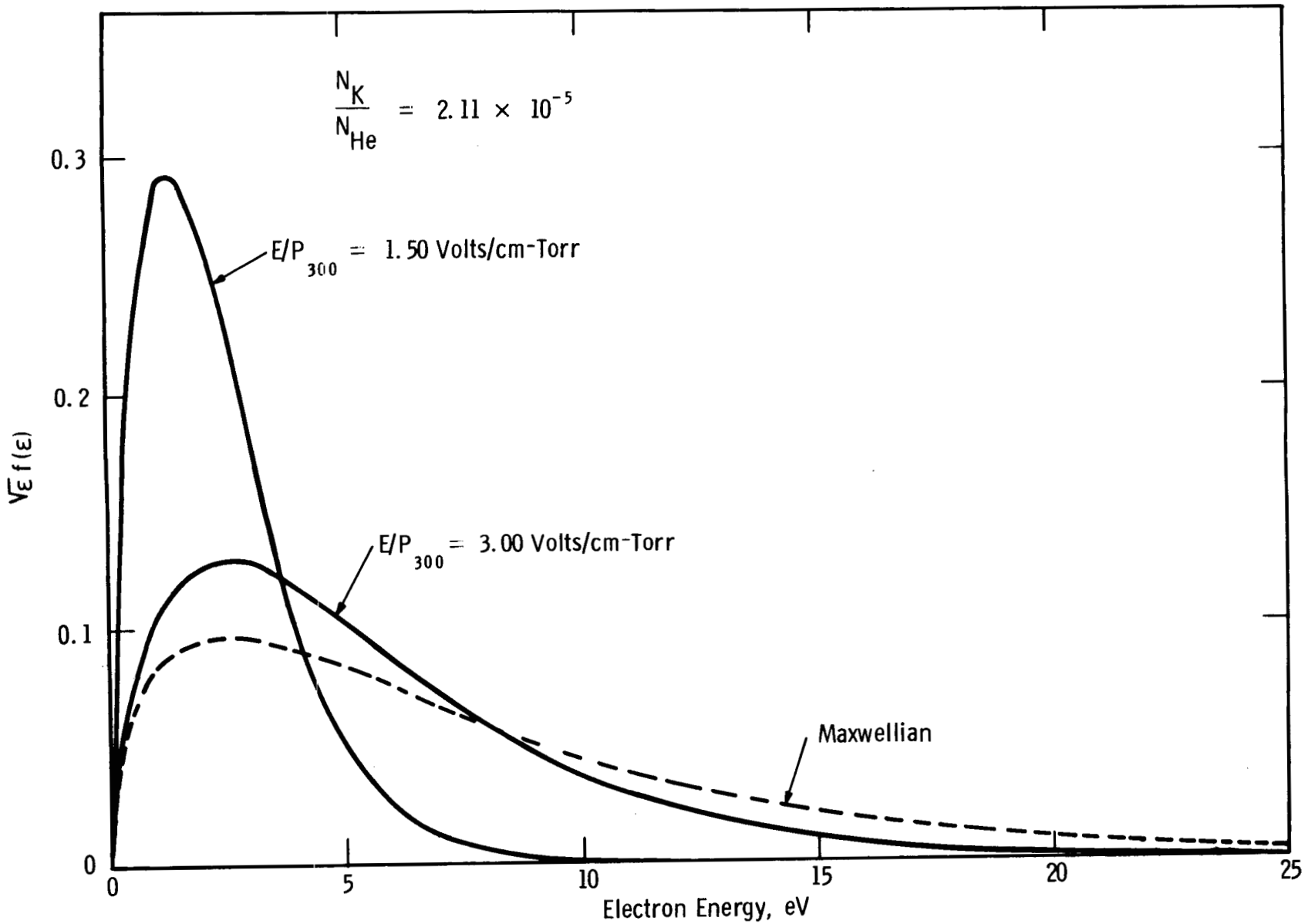

Fig. 7 Electron energy distribution functions for two values of E/p_{300}. Also shown for comparison is a Maxwellian distribution function (dotted curve) with a peak energy equal to that of the calculated distribution function for E/p_{300} = 3.0 Volts/cm-Torr.

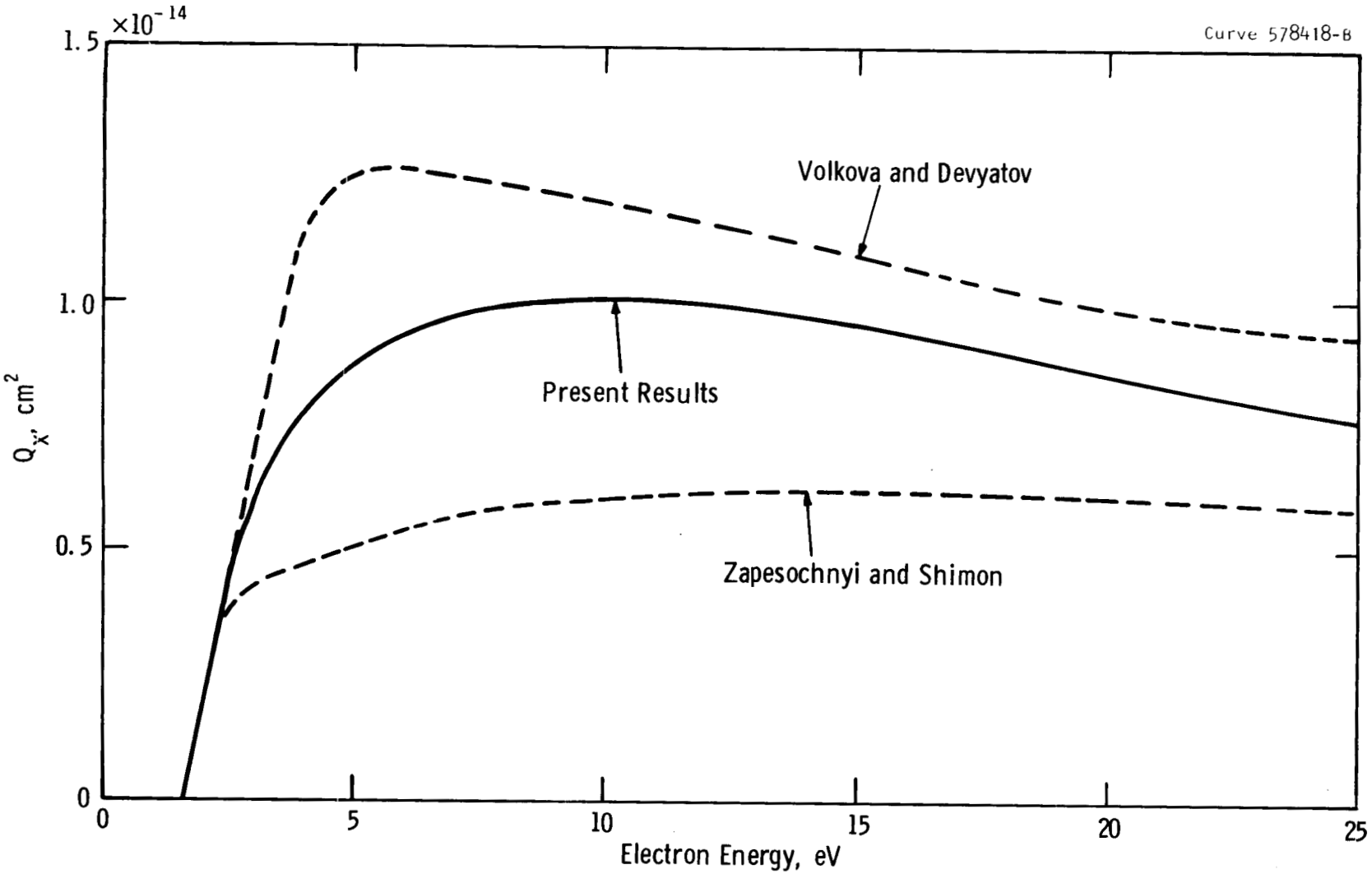

Fig. 8 Comparison of the total potassium excitation cross section derived from the present work with the cross section for 4S-4P excitation as found by Volkova and Devyatov (reference 11) and by Zapesochnyi and Shimon (reference 12).

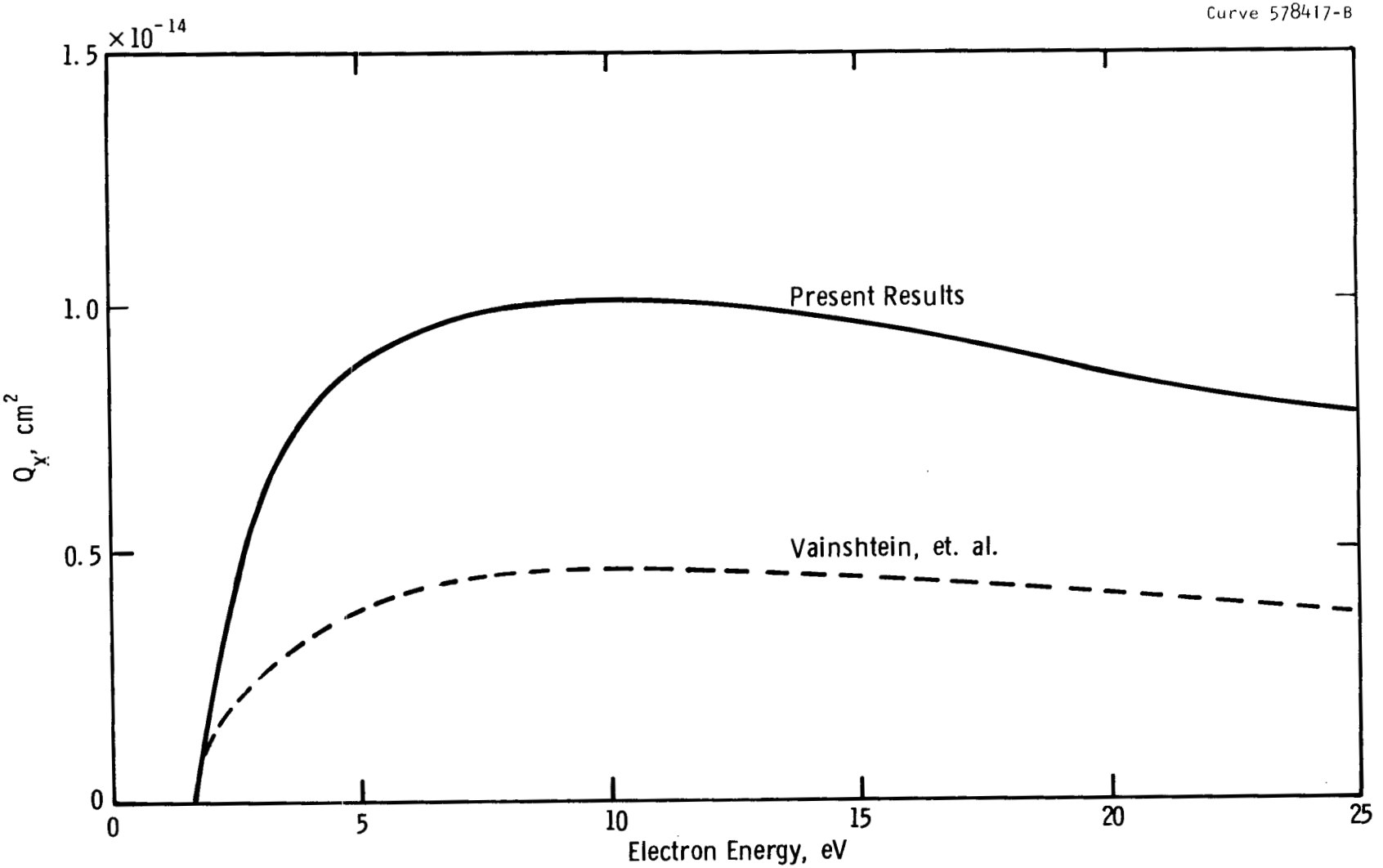

Fig. 9 Comparison of the theoretical cross section for 4S-4P potassium excitation as found by Vainshtein et al (reference 13) with the present results.

DISTRIBUTION LIST FOR CONTRACT NAS3-7930

FINAL REPORT

	Addressee	Number of Copies
1.	National Aeronautics and Space Administration Washington, D. C. 20546	
	Attn: RNT/James Lazar	2
	RNT/Jerry Mullin	1
	RPE/Dr. H. Harrison	1
	RNP/Dr. F. Schulman	1
	RNP/J. Lynch	2
	RNP/Dr. K. H. Thom	1
2.	NASA-Lewis Research Center 21000 Brookpark Road Cleveland, Ohio 44135	
	Attn: Spacecraft Technology Procurement Section M.S. 54-2	1
	C. C. Conger M.S. 54-1	1
	N. J. Stevens M.S. 54-3	5
	Bernard Lubarsky	2
	H. Nastelin	1
	L. D. Nichols	1
	Dean Kaul	1
	John Sheldon	1
	W. E. Moeckel	1
	G. R. Seikel	1
	Technology Utilization Officer M.S. 3-19	1
	Library M.S. 60-3	2
	Report Control Office M. S. 5-5	1
3.	Office of Naval Research Power Branch (Code 429) Washington, D. C. 20025	
	Attn: Dr. Ralph Roberts	1
	John Satkowski/Room 2509	1
4.	Aeronautical Systems Division Flight Accessories Laboratory Wright-Patterson AFB, Ohio 45433	
	Attn: Robert Barthelemy, APIE-2	2
5.	U. S. Air Force Office of Scientific Research Washington, D. C. 20025	
	Attn: Dr. M. Slawsky	1

CONTRACT NAS3-7930

	Addressee	Number of Copies
6.	AVCO/Everett Research Laboratory 2385 Revere Beach Parkway Everett, Massachusetts 02149 Attn: T. Brogan	1
7.	Electrical Engineering Department Massachusetts Institute of Technology Cambridge, Massachusetts 02139 Attn: Dr. J. Kerrebrock Prof. H. H. Woodson	1 1
8.	MHD Research, Inc. 1535 Monrovia Street Newport Beach, California 92661 Attn: Dr. V. H. Blackman	1
9.	General Atomic Division General Dynamics Corporation P. O. Box 608 San Diego, California 92112 Attn: Dr. J. Colwell	1
10.	Martin-Marietta Corporation Baltimore, Maryland 21203 Attn: Dr. Bienert	1
11.	Aerospace Corporation P. O. Box 95085 Los Angeles, California 90045 Attn: Library Technical Documents Group	1
12.	Hughes Research Laboratories Plasma Physics Department 3011 Malibu Canyon Road Malibu, California 93032 Attn: R. C. Knechtli	1
13.	Stanford University M. E. Department Stanford, California 94305 Attn: Dr. R. Eustis	1
14.	General Electric Company Missile and Space Division Valley Forge Space Technology Center P. O. Box 8555 Philadelphia, Pennsylvania 19101 Attn: Dr. A. Sherman	1

CONTRACT NAS3-7930

	Addressee	Number of Copies
15.	American-Standard Research Division New Brunswick, New Jersey 08903 Attn: E. Okress	1
16.	Jet Propulsion Laboratory California Institute of Technology 4800 Oak Grove Drive Pasadena, California ; 91103	1
17.	California Institute of Technology Chemical Engineering Department Pasadena, California 91109 Attn: Dr. F. Shair	1
18.	General Dynamics Corporation General Dynamics/Convair P. O. Box 1128 San Diego, California 92112 Attn: Dr. A. Larson	1
19.	Electro-Optical Systems, Inc. 300 North Halstead Street Pasadena, California 91107 Attn: Dr. Gordon Cann	1
20.	NASA Scientific and Technical Information Facility P. O. Box 33 College Park, Maryland 20740 Attn: RQT-2448/NASA Representative	6
21.	AFWL Kirtland AFB, New Mexico 87417 Attn: WLPC/Capt. C. F. Ellis	1
22.	AVCO Research and Advanced Development Division 201 Lowell Street Wilmington, Massachusetts 01887 Attn: Dr. R. John	1
23.	University of California at San Diego Physics Department San Diego, California 92110 Attn: Dr. Ralph Lovberg	1

CONTRACT NAS3-7930

	Addressee	Number of Copies
24.	Westinghouse Astronuclear Laboratories Electric Propulsion Laboratory Pittsburgh, Pennsylvania 15234 Attn: Library	1
25.	Atomics International 8900 DeSoto Avenue Canoga Park, California 91304 Attn: Dr. Guderjahn Dept. 742	1
26.	Institute for Aerospace Studies University of Toronto Toronto 5, Canada Attn: Dr. Stanley J. Townsend	1